# Communication: The influence of CO2 poisoning on overvoltages and discharge capacity in non-aqueous Li-Air batteries

**Mekonnen, Yedilfana Setarge; Knudsen, Kristian Bastholm; Mýrdal, Jón Steinar Garðarsson; Younesi, Reza; Højberg, Jonathan; Hjelm, Johan; Norby, Poul; Vegge, Tejs**

*Published in:*
Journal of Chemical Physics

*Link to article, DOI:*
10.1063/1.4869212

*Publication date:*
2014

*Document Version*
Publisher's PDF, also known as Version of record

# Communication: The influence of CO2 poisoning on overvoltages and discharge capacity in non-aqueous Li-Air batteries

Yedilfana S. Mekonnen, Kristian B. Knudsen, Jon S. G. Mýrdal, Reza Younesi, Jonathan Højberg, Johan Hjelm, Poul Norby, and Tejs Vegge

Citation: The Journal of Chemical Physics **140**, 121101 (2014); doi: 10.1063/1.4869212
View online: http://dx.doi.org/10.1063/1.4869212
View Table of Contents: http://scitation.aip.org/content/aip/journal/jcp/140/12?ver=pdfcov
Published by the AIP Publishing

# Communication: The influence of $CO_2$ poisoning on overvoltages and discharge capacity in non-aqueous Li-Air batteries

Yedilfana S. Mekonnen,[1,2] Kristian B. Knudsen,[1] Jon S. G. Mýrdal,[1] Reza Younesi,[1] Jonathan Højberg,[1] Johan Hjelm,[1] Poul Norby,[1] and Tejs Vegge[1,a)]
[1]*Department of Energy Conversion and Storage, Technical University of Denmark, Frederiksborgvej 399, DK-4000 Roskilde, Denmark*
[2]*Center for Atomic-scale Materials Design, Technical University of Denmark, DK-2800 Lyngby, Denmark*

(Received 31 January 2014; accepted 11 March 2014; published online 24 March 2014)

The effects of $Li_2CO_3$ like species originating from reactions between $CO_2$ and $Li_2O_2$ at the cathode of non-aqueous Li-air batteries were studied by density functional theory (DFT) and galvanostatic charge-discharge measurements. Adsorption energies of $CO_2$ at various nucleation sites on a stepped $(1\bar{1}00)$ $Li_2O_2$ surface were determined and even a low concentration of $CO_2$ effectively blocks the step nucleation site and alters the $Li_2O_2$ shape due to $Li_2CO_3$ formation. Nudged elastic band calculations show that once $CO_2$ is adsorbed on a step valley site, it is effectively unable to diffuse and impacts the $Li_2O_2$ growth mechanism, capacity, and overvoltages. The charging processes are strongly influenced by $CO_2$ contamination, and exhibit increased overvoltages and increased capacity, as a result of poisoning of nucleation sites: this effect is predicted from DFT calculations and observed experimentally already at 1% $CO_2$. Large capacity losses and overvoltages are seen at higher $CO_2$ concentrations. © *2014 AIP Publishing LLC*. [http://dx.doi.org/10.1063/1.4869212]

## I. INTRODUCTION

As energy storage needs are growing rapidly, there is also an increase in research into high energy density materials for energy storage. Significant attention has been given to metal-air batteries, particularly Li-air batteries, as future environmentally friendly high energy density storage for vehicles, where the capacity offered by existing Li-ion technology is too low to solve the increasing demands on batteries.[1] The Li-$O_2$ couple is particularly attractive and could have ∼5–10 times greater specific energies than currently available Li-ion batteries, though there are severe scientific and technical challenges that need to be addressed.[2,3] Such as a clear understanding of the $Li_2O_2$ growth mechanisms, transport processes, interfacial phenomena, air impurities, and stability of the key components are vital parts of non-aqueous rechargeable Li-air cell research.[4]

As first reported by Abraham and Jiang in 1996, the Li-$O_2$ battery with aprotic solvent is shown to be rechargeable, when $Li_2O_2$ is formed during discharge at the cathode.[5] Detailed understanding of the $Li_2O_2$ growth mechanism is important to solve the problem associated with the practical limitations of the battery. Previous theoretical works by Hummelshøj *et al.*[6] and Radin *et al.*[7,8] showed that steps on a reconstructed $(1\bar{1}00)$surface could act as nucleation sites for low discharge overvoltage and facets such as (0001), $(1\bar{1}00)$, and $(11\bar{2}0)$ have similar surface energies. Hummelshøj *et al.*[9] have also shown that surfaces are potential dependent and vary during discharge and charge. According to $G_0W_0$ calculations, both $Li_2O_2$ and $Li_2CO_3$ are insulating materials with wide band gap of 4.9 and 8.8 eV, respectively.[10–12] Therefore, as these materials deposit at the cathode surface during discharge they will limit the electronic conduction and lead to sudden death during discharge within 5–10 nm thick $Li_2O_2$ deposits.[13,14] However, recent DFT calculations found that hole and electron polaronic transports at the surface and in bulk $Li_2O_2$ and $Li_2CO_3$ can take place. Using a PBE+U (Hubbard-corrected Perdew–Burke–Ernzerhof) exchange correlation functional, Garcia-Lastra *et al.*[11] revealed that the hole polarons have higher mobility than electron polarons and $Li_2CO_3$ exhibits lower conduction than $Li_2O_2$. Recent works by Luntz *et al.* have shown that hole tunneling should dominate and polaronic transport is only expected to be significant in $Li_2O_2$ at elevated temperatures and low current densities.[15,16]

$Li_2CO_3$ like crystalline species are formed by parasitic side reactions between the $Li_2O_2$ or $LiO_2$ and carbon sources from air impurities such as CO and $CO_2$ gases,[17] the graphite itself, or the decomposition of aprotic electrolytes. Younesi *et al.*[18,34] reported the degradation of various electrolytes by $Li_2O_2$ and documented $Li_2CO_3$ as a decomposition product from aprotic electrolytes. Likewise, McCloskey *et al.*[3] have shown that carbonates accumulate at the C-$Li_2O_2$ and $Li_2O_2$-electrolyte interfaces and are responsible for a large potential increase during recharge and a huge decrease in exchange current density. This makes growth of $Li_2O_2$ on $Li_2CO_3$ an equally important process to investigate, but this is beyond the scope of this communication. As reported by Siegfried *et al.*[19] and Myrdal and Vegge[20] adsorption of sulfur containing compounds on oxide surfaces could also control the electrochemical growth mechanism. Adsorbed species at surfaces can potentially block the nucleation sites, and therefore, alter the growth directions, overvoltages, and capacities.

In this communication, we address the influence of $CO_2$ contamination on the $Li_2O_2$ growth mechanism, discharge/charge overvoltages, and capacity in non-aqueous

a)E-mail: teve@dtu.dk

 

TABLE I. Adsorption energies of $CO_2$ in the gas phase at $(1\bar{1}00)$ $Li_2O_2$ surface.

| Species | Sites | Adsorption energy (eV) |
|---|---|---|
| $CO_2$ | Step valley | −0.73 |
| | Terrace valley | −0.21 |
| | Step ridge | −0.02 |

Li-air batteries using density functional theory (DFT) and galvanostatic measurements. Among other air contaminants, $CO_2$ is the most critical subject due to its high solubility in aprotic electrolytes and high reactivity with $Li_2O_2$ to form an insulating material $Li_2CO_3$.

## II. COMPUTATIONAL RESULTS AND ANALYSIS

DFT[21–23] as implemented in the GPAW (grid-based projector-augmented wave method) code[24] is used to perform the presented calculations through the atomic simulation environment (ASE).[25] GPAW is built on real space grids and non-valence electrons are described by PAW (projector augmented-wave method).[26,27] Electron exchange and correlation is approximated by the revised Perdew–Burke–Ernzerhof (RPBE) functional.[28] The stepped $(1\bar{1}00)$ $Li_2O_2$ surface with a super cell consisting of a 56–64 atoms slab with a 18 Å vacuum layer between periodic images along the z-axis, see Fig. S1 in the supplementary material.[35] Since the oxygen rich (0001) facet will also be exposed, in particular under charging conditions,[9] and subsequent investigations should be performed to analyze the detailed mechanisms of $CO_2$ bonding to this facet. Recent computational DFT results for $SO_2$ adsorption on stepped (0001) and $(1\bar{1}00)$ surfaces do, however, show preferential bonding to the $(1\bar{1}00)$ facets,[20] which is investigated here. The k-points are sampled with a (4,4,1) Monkhorst-Pack mesh and 0.15 grid points is used. Atomic energy optimization calculations are performed until all forces are less than 0.01 eV/Å. Energy barriers are calculated by the climbing image nudged elastic band (CINEB) method.[29–31]

Adsorption energies of $CO_2$ at various nucleation sites on a stepped $(1\bar{1}00)$ $Li_2O_2$ surface were determined, see Table I. $CO_2$ binds preferentially at the step valley site and weakly binds at the step ridge site. NEB calculations show that once $CO_2$ is adsorbed at step valley site, it is bound by barriers upwards of 3 eV, see Fig. S2 in the supplementary material,[35] since the $CO_2$ molecule is required to desorb from the surface prior to re-adsorbing at the step site. The detailed nature of a conversion of adsorbed $CO_2$ to $Li_2CO_3$ warrants further investigations, but we find the adsorption of a single $CO_2$ molecule forms a $Li_{\sim 3}CO_3$-type complex (Fig. 1(b)), which could act as a nucleation site for further growth of $Li_2CO_3$.

The computational lithium electrode approach is used in the free energy calculations.[6,32] Defined as, U = 0, when bulk Li anode and Li ions in solution ($Li^+ + e^-$) are at equilibrium. The free energy change of the reaction is shifted by $-neU$ at an applied bias, where $n$ is the number of transferred electrons; other assumptions are listed in the supplementary material.[35] As reported by Hummelshøj *et al.*, kinks and steps sites of the stepped $(1\bar{1}00)$ $Li_2O_2$ surface are favorable nucleation sites for a low overvoltage $Li_2O_2$ growth mechanism. The influence of $CO_2$ poisoning on the $Li_2O_2$ growth mechanism is studied while $CO_2$ is already adsorbed at step valley site (Fig. 1(b)).

The free energy diagram in Fig. 2 shows a four steps, two formula units $Li_2O_2$ growth mechanism on the stepped $(1\bar{1}00)$ $Li_2O_2$ surface with and without $CO_2$. The first step in the presence of $CO_2$ is adsorption of $LiO_2$ species (Fig. 1(c)), and which reduces the binding energy by 0.44 V compared to the pure discharge. The next step is the addition of a second $LiO_2$ species (Fig. 1(d)), which is the potential limiting charge step that raises the binding energy by 0.20 V compared to pure $Li_2O_2$. This is followed by subsequent additions of two Li (Figs. 1(e) and 1(f)) with relatively small binding energies with respect to a pure discharge. In the pure $O_2$ discharge mechanism, unlike in the presence of $CO_2$, addition of the first Li is the limiting charge potential step. The $2Li_2O_2$ growth at the step surface effectively displaces $CO_2$ from the step to the less stable terrace site.

Hummelshøj *et al.* have reported that the pure $Li_2O_2$ growth mechanism follows a 4 steps reaction mechanism, where all reaction steps are electrochemical, similar to what is seen in the presence of $CO_2$. The equilibrium potential can be obtained as $U_0 = -\Delta G/2e$. The effective equilibrium potential on a pure surface becomes 2.73 V (experimental value, $U_{0,Exp} = 2.85$ V), while in the presence of $CO_2$, this is effectively reduced to 2.53 V for the first cycle due to the shift in binding energy of $CO_2$ from a step valley to terrace site. As a result, discharge at other facets may become activate.[9] At neutral bias all reaction steps are downhill, but at an applied potential, the free energy difference changes for each step calculated as

$$\Delta G_{i,U} = \Delta G_i - eU. \quad (1)$$

The lowest free energy step, $\Delta G_{i,min}$, along the reaction path becomes uphill first at an applied potential called limited discharge potential, $U_{discharge}$, while the largest free energy step, $\Delta G_{i,max}$, that is last to become downhill for the reversed reaction at an applied potential called limited charge potential, $U_{charge}$, obtained as

$$U_{discharge} = \min[-\Delta G_i/e] \text{ and } U_{charge} = \max[-\Delta G_i/e]. \quad (2)$$

In the presence (absence) of a single $CO_2$ molecule, this discharge occurs as described in Fig. 1, resulting in $U_{discharge}$ = 2.21 V (2.66 V), and $U_{charge}$ = 2.97 V (2.81 V) and the discharge and charge overvoltages in the presence (absence) of $CO_2$ are $\eta_{discharge} = 0.31$ V (0.07 V), and $\eta_{charge} = 0.44$ V (0.08 V). The calculated 0.44 V overvoltage for charge corresponds to low $CO_2$ concentrations, where only a single $CO_2$ molecule is adsorbed on the $Li_2O_2$ step forming a $Li_{\sim 3}CO_3$ type complex (see Fig. 1). Here, the charging process follows the same reaction steps as the discharge, but in reverse (from right to left in Fig. 2), i.e., the first two steps are desorption of two Li and followed by desorption of 2 $LiO_2$ species: in total desorbing 2 $Li_2O_2$ units from the surface and returning to the configuration in Fig. 1(b). Quantitative agreement with

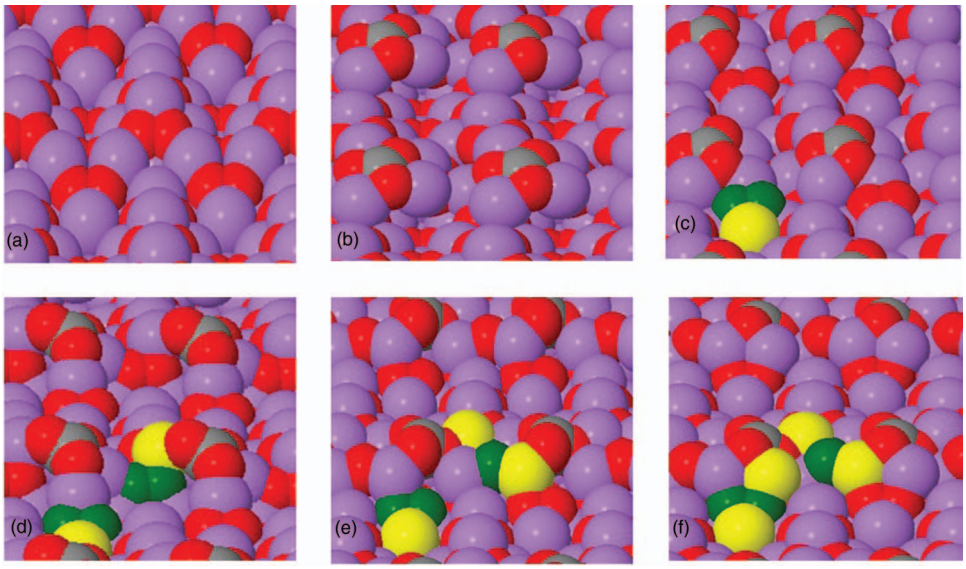


FIG. 1. Stepped $Li_2O_2$ ($1\bar{1}00$) surface before and after adsorption of $CO_2$ and 4 steps $Li_2O_2$ growth pathways during discharge. (a) Pure stepped $Li_2O_2$ surface. (b) $CO_2$ adsorbs to step valley site forming a $Li_{\sim 3}CO_3$ type complex. (c) 1st $LiO_2$ adsorbs. (d) 2nd $LiO_2$ adsorbs. (e) 1st Li. (f) 2nd Li adsorbs to the surface completing growth of 2 $Li_2O_2$ formula units. Atoms labeled as: C (gray), Li (purple), and O (red). Deposited atoms shown as: Li (yellow) and O (green).

experimental overvoltages can therefore only be expected for low concentrations of $CO_2$ (e.g., 1%). For higher $CO_2$ concentrations, the formation of crystalline $Li_2CO_3$ would be expected, resulting in significantly larger overvoltages.[3]

## III. EXPERIMENTAL RESULTS AND ANALYSIS

Li-air batteries were constructed using a Swagelok design and assembled inside an Ar-filled glovebox ($\leq$3 ppm $O_2$ and $H_2O$). Each battery contained a 200 $\mu$l 1 M LiTFSI (99.95%, Sigma-Aldrich) and 1,2-dimethoxymethane, DME, ($H_2O$ < 20 ppm, BASF) electrolyte. Cathodes consisted of P50 AvCarb carbon paper (Fuel cell store), which were sonicated using 2-propanol (99.5%, Sigma-Aldrich) and acetone ($\geq$99.8%, Sigma-Aldrich), introduced into a glovebox where they were rinsed with DME before drying in vacuum at 80 °C for 12 h. Cathodes were supported by a 316 steel mesh. A 10 mm diameter lithium foil (99.9%, Sigma-Aldrich) was used as anode. Two Celgard separators 2500 (Celgard) were placed in between the two electrodes. The separators were sonicated in EtOH (99.9%, Sigma-Aldrich), transferred to a glovebox, and rinsed with DME before drying in vacuum at 80 °C for 12 h. Experiments were performed using a Bio-Logic VMP3 Multichannel galvanostat (Bio-Logic, Claix, France). Batteries were operated in two galvanostatic modes: First, at 100 $\mu$A (127.3 $\mu$A/cm$^2$) where cells were discharged to 2 V and charged to 4.6 V vs. $Li^+$/Li. Second, at 50 $\mu$A (63.6 $\mu$A/cm$^2$) using the same potential limits.

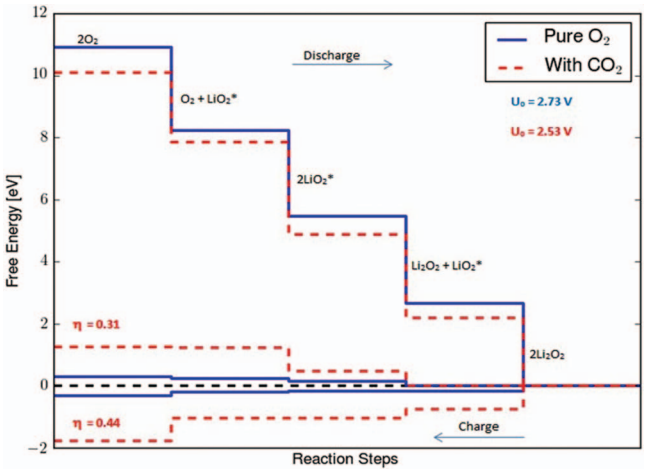


FIG. 2. Calculated free energy diagrams for a four steps discharge mechanism on a stepped ($1\bar{1}00$)$Li_2O_2$ surface with and without adsorbed $CO_2$.

To investigate the effect of gaseous $CO_2$, the assembled cells were purged with three different atmospheres: 0/100 $CO_2/O_2$, 1/99 $CO_2/O_2$, and 50/50 $CO_2/O_2$. Three individual batteries were assembled and investigated for each atmosphere and each curve presented in Figs. 3 and 4 is therefore an average of three cells with the equal atmosphere as shown in Fig. S3 in the supplementary material.[35] The lowest discharge capacity was observed for the 50% $CO_2$ cells and is likely caused by the high concentration of electrochemically inactive $CO_2$. A similar effect was observed, by Gowda *et al.*[17] for a pure $CO_2$ cell, where the cell potential immediately dropped. It should however be noted that Takechi *et al.*[33] observed, quite to the contrary of our observations, higher discharge capacities up to 70% $CO_2$ with respect to pure $O_2$ cells. Interestingly, a higher discharge capacity was observed for the 1% $CO_2$ cells in respect to the pure $O_2$ cells as shown in Fig. 3 (inset). A possible explanation is the dissolution of $Li_2CO_3$ species in DME and/or, as also suggested by Gowda *et al.*, or a change in deposition morphology compared to that deposited in the pure $O_2$ cells as suggested by Myrdal and Vegge.[20] Such morphological changes could increase the total electrodeposited layer and lead to higher capacities.

All $CO_2$ cells have higher discharge overvoltages compared to cells with pure $O_2$ at a discharge rate of 127.3 $\mu$A/cm$^2$, which may be caused by the blocking of the

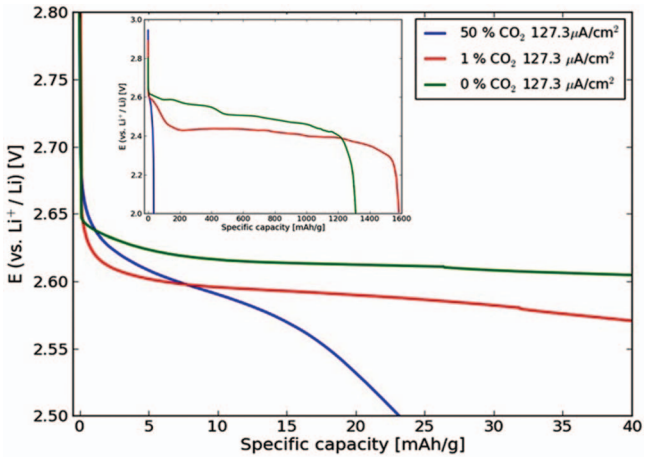


FIG. 3. Galvanostatic discharge profiles at 127.3 $\mu$A/cm$^2$ discharge at three different atmospheres: 50% $CO_2$, 1% $CO_2$, and 0% $CO_2$. Inset shows the increase in discharge capacity in 1% $CO_2$.

active nucleation sites by solubilized $CO_2$, forcing the reactions to follow pathways with higher overvoltages. This effect can even be seen at 1% $CO_2$, as illustrated in Fig. 3 above. The charge capacity, as seen in Fig. 4 and Fig. S4 in the supplementary material,[35] is very dependent on the $CO_2$ concentration, with high concentrations limiting charge capacity and thereby the cell reversibly. The 50% $CO_2$ cells reach the lower potential limit (2.0 V) early, at approximately 35 mAh/g, while 1% $CO_2$ cells and pure $O_2$ cells continued until capacities in the range 1150–1600 mAh/g were reached depending on current density. The low charge capacity at high $CO_2$ contaminations should be attributed to the poor Li-$CO_2$ electrochemistry, also reported by Gowda *et al.* The charging overvoltages are a function of both current density and the level of $CO_2$ contamination. While there is no significant difference in overvoltages between cells charge at 127.3 and 63.6 $\mu$A/cm$^2$ for 50% $CO_2$ cells, which again can be attributed to the poor Li-$CO_2$ electrochemistry. At 127.3 $\mu$A/cm$^2$, there is an increase in overvoltage of about 0.4 and 0.3 V for 1% $CO_2$ cells and 0% $CO_2$ cells, respectively. The general increase in overvoltages with increasing current density can be explained

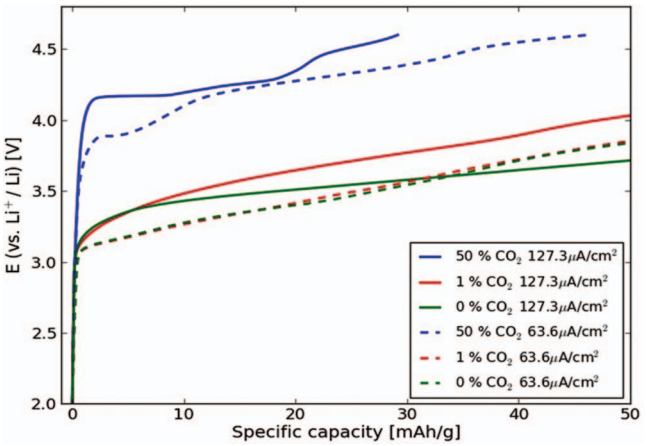


FIG. 4. Galvanostatic charge profiles at 127.3 (solid) and 63.6 (dotted) $\mu$A/cm$^2$ at three different atmospheres: 50% $CO_2$, 1% $CO_2$, and 0% $CO_2$.

by the Butler-Volmer model, while the larger overvoltage for the 1% $CO_2$ cells than 0% $CO_2$ cells is expectedly caused by the formation and oxidation of the carbonate like species (Fig. 1(b)). A second charge at 63.6 $\mu$A/cm$^2$ shows identical results for 1% and 0% $CO_2$. This can be ascribed to the evolution of $CO_2$ observed during the initial charge cycle, where $CO_2$ is released at 4.5 V, as shown in Fig. S5 in the supplementary material,[35] resulting in residual $CO_2$ in the electrolyte causing blocking of the step sites in subsequent charging experiments.

## IV. CONCLUSIONS

Influences of $CO_2$ poisoning at a stepped (1$\bar{1}$00) $Li_2O_2$ surface in non-aqueous Li-air battery were studied using DFT calculations and cells were characterized by electrochemical charge-discharge measurements. $CO_2$ preferentially binds at step valley site at the $Li_2O_2$ surface and the $Li_2O_2$ growth mechanism consists of four electrochemical steps, following the same sequence for both pure and contaminated systems. Accordingly, the first step of the growth mechanism is the adsorption of two $LiO_2$ species and followed by addition of two Li to form 2 $Li_2O_2$ at the cathode surface. For charge in the low $CO_2$ limit, a similar reaction will occur, but in reverse order.

Low concentrations of $CO_2$ (1%) effectively block the surface-active nucleation sites and alter the shape and growth directions of $Li_2O_2$ on the surface; resulting in an increased capacity of the battery at the expense of an increase in the overvoltage in the presence of $CO_2$. A similar behavior is seen in pure oxygen following charging to 4.5 V, resulting from decomposition reactions. The effective discharge potential is reduced by 0.20 V on a stepped (1$\bar{1}$00) $Li_2O_2$ surface, shifting the reaction to alternate nucleation sites. In general, the DFT calculations and experimental results show that the recharging process is strongly influenced by $CO_2$ contamination, and exhibits significantly increased charging overvoltage, which is observed already with 1% $CO_2$ contamination, while at 50% $CO_2$ a large capacity loss is also seen.

## ACKNOWLEDGMENTS

The authors acknowledge support of this work from the ReLiable project (Project No. 11-116792) funded by the Danish Council for Strategic Research Programme Commission on Sustainable Energy and Environment.

[1]D. Linden and T. Reddy, *Hand Book of Batteries*, 3rd ed. (McGraw Hill, New York, 2001).
[2]T. Ogasawara, A. Débart, M. Holzapfel, P. Novák, and P. G. Bruce, J. Am. Chem. Soc. **128**, 1390 (2006).
[3]B. D. McCloskey, A. Speidel, R. Scheffler, D. C. Miller, V. Viswanathan, J. S. Hummelshøj, J. K. Nørskov, and A. C. Luntz, J. Phys. Chem. Lett. **3**, 997 (2012).
[4]G. Girishkumar, B. D. McCloskey, A. C. Luntz, S. Swanson, and W. Wilcke, J. Phys. Chem. Lett. **1**, 2193 (2010).
[5]K. M. Abraham and Z. Jiang, J. Electrochem. Soc. **143**, 1 (1996).
[6]J. S. Hummelshøj, J. Blomqvist, S. Datta, T. Vegge, J. Rossmeisl, K. S. Thygesen, A. C. Luntz, K. W. Jacobsen, and J. K. Nørskov, J. Chem. Phys. **132**, 071101 (2010).
[7]M. D. Radin, J. F. Rodriguez, F. Tian, and D. J. Siegel, J. Am. Chem. Soc. **134**, 1093 (2011).

[8]M. D. Radin, F. Tian, and D. J. Siegel, J. Mat. Sci. **47**, 7564 (2012).
[9]J. S. Hummelshøj, A. C. Luntz, and J. K. Nørskov, J. Chem. Phys. **138**, 034703 (2013).
[10]P. Albertus, G. Girishkumar, B. D. McCloskey, R. S. Sanchez-Carrera, B. Kozinsky, J. Christensen, and A. C. Luntz, J. Electrochem. Soc. **158**(3), A343 (2011).
[11]J. M. Garcia-Lastra, J. S. G. Myrdal, K. S. Thygesen, and T. Vegge, J. Phys. Chem. C **117**, 5568 (2013).
[12]J. M. Garcia-Lastra, J. D. Bass, and K. S. Thygesen, J. Chem. Phys. **135**, 121101 (2011).
[13]V. Viswanathan, K. S. Thygesen, J. S. Hummelshøj, J. K. Nørskov, G. Girishkumar, B. D. McCloskey, and A. C. Luntz, J. Chem. Phys. **135**, 214704 (2011).
[14]J. Chen, J. S. Hummelshøj, K. S. Thygesen, J. S. G. Myrdal, J. K. Nørskov, and T. Vegge, Catal. Today **165**, 2 (2011).
[15]J. B. Varley, V. Viswanathan, J. K. Nørskov, and A. C. Luntz, Energy Environ. Sci. **7**, 720 (2014).
[16]A. C. Luntz, V. Viswanathan, J. Voss, J. B. Varley, J. K. Nørskov, R. Scheffler, and A. Speidel, J. Phys. Chem. Lett. **4**, 3494 (2013).
[17]S. R. Gowda, A. Brunet, G. M. Wallraff, and B. D. McCloskey, J. Phys. Chem. Lett. **4**, 276 (2013).
[18]R. Younesi, M. Hahlin, F. Björefors, P. Johansson, and K. Edström, Chem. Mater. **25**, 77 (2013).
[19]M. J. Siegfried and K. S. Choi, Adv. Mat. **16**, 1743 (2004).
[20]J. S. G. Myrdal and T. Vegge, "DFT study of selective poisoning of Li-Air batteries for increased discharge capacity," RSC Adv. (to be published).
[21]P. Hohenberg and W. Kohn, Phys. Rev. **136**, B864 (1964).
[22]W. Kohn and L. Sham, Phys. Rev. **140**, A1133 (1965).
[23]J. J. Mortensen, L. B. Hansen, and K. W. Jacobsen, Phys. Rev. B **71**, 035109 (2005).
[24]J. Enkovaara, C. Rostgaard, J. J. Mortensen, J. Chen, M. Dulak, L. Ferrighi, J. Gavnholt, C. Glinsvad, V. Haikola, H. A. Hansen, H. H. Kristoffersen, M. Kuisma, A. H. Larsen, L. Lehtovaara, M. Ljungberg, O. Lopez-Acevedo, P. G. Moses, J. Ojanen, T. Olsen, V. Petzold, N. A. Romero, J. Stausholm-Moller, M. Strange, G. A. Tritsaris, M. Vanin, M. Walter, B. Hammer, H. Hakkinen, G. K. H. Madsen, R. M. Nieminen, J. K. Nørskov, M. Puska, T. T. Rantala, J. Schiøtz, K. S. Thygesen, and K. W. Jacobsen, J. Phys. Condens. Matter **22**, 253202 (2010).
[25]S. R. Bahn and K. W. Jacobsen, Comput. Sci. Eng. **4**, 56 (2002).
[26]P. E. Blöchl, Phys. Rev. **50**, 17953 (1994).
[27]P. E. Blöchl, C. J. Först, and J. Schimpl, Bull. Mater. Sci. **26**, 33 (2003).
[28]B. Hammer, L. B. Hansen, and J. K. Nørskov, Phys. Rev. B **59**, 7413 (1999).
[29]H. Jonsson, G. Mills, and K. W. Jacobsen, *Classical and Quantum Dynamics in Condensed Phase Systems*, edited by B. J. Berne, G. Cicotti, and D. F. Coker (World Scientific, 1998).
[30]G. Henkelman and H. Jónsson, J. Chem. Phys. **113**, 9978 (2000).
[31]G. Henkelman, B. Uberuaga, and H. A. Jónsson, J. Chem. Phys. **113**, 9901 (2000).
[32]J. K. Nørskov, J. Rossmeisl, A. Logadottir, L. Lindqvist, J. R. Kitchin, T. Bligaard, and H. Jonsson, J. Phys. Chem. B **108**, 17886 (2004).
[33]K. Takechi, T. Shiga, and T. Asaoka, Chem. Commun. **47**, 3463 (2011).
[34]R. Younesi, P. Norby, and T. Vegge, ECS Electrochem. Lett. **3**, A15 (2014).
[35]See supplementary material at http://dx.doi.org/10.1063/1.4869212 for Figs. S1–S5.